International Journal of Signal Processing, Image Processing and Pattern Recognition
Vol.6, No.5 (2013), pp.153-164
http://dx.doi.org/10.14257/ijsip.2013.6.5.14

# A Hierarchical Segmentation Approach towards Roads and Slopes for Collapse Recognition

Yuanyuan Jia[1], Zhongshi He[1] and Huazheng Zhu[1]

[1]*College of Computer Science, Chongqing University, Chongqing, 400044-China*
*yyjia@cqu.edu.cn, zshe@cqu.edu.cn, huazhengzhu@cqu.edu.cn*

***Abstract***

*Color image processing is widely used in Intelligent Transport System, but seldom used in recognition of roads and slopes collapse. The application can reduce time and efforts. And the roads and slopes segmentation is the first and key step of the recognition system, which is a challenging and difficult problem. One of the problems is the presence of different types of roads and slopes. In this paper, we propose a novel framework for segmenting road images in a hierarchical manner that can separate the following objects: road and slopes with or without collapse, sky, road signs, cars, buildings and vegetation from the images. Then the Region of Interests (ROIs), i.e. the roads and slopes, are obtained with the geometrical, location of the objects and statistical color features which are extracted based on L*a*b color space and Gabor filter. According to combination K-means clustering with region merging, connected-component algorithm and morphological operation, the roads and slopes are segmented. The hierarchical approach does not assume the roads are present in the same type and assume the road images can be captured from arbitrary angles. The experiments show that the approach in this paper can achieve a satisfied result on various road images.*

***Keywords:*** *Road image segmentation; Gabor filter; color feature; K-means clustering; roads and slopes collapse*

## 1. Introduction

Research into intelligent transportation systems (ITSs) has seen considerable development over the last few decades. ITSs are various: including driving-assistance systems [1], detection of obstacles [2-4], road scene understanding [5], road signs detection [6] and roads disease detection in which the color image processing plays an important role. This paper is focus on the field of the roads disease detection based on color image processing. Most of the previous works for road diseases are about road crack detection [7, 8]. However, few people utilize color image processing to recognize roads and slopes collapse.

Recently, increasing accidents have happened because of the collapse. So the roads and slopes must be monitored to discover collapse, and prevent accidents. However, it is time-consuming and inefficient to inspect the roads and slopes by human. So cameras can be installed beside the roads for acquisition images of roads and slopes automatically. Then the images are sent to the data processing center and collapse will be recognized base on colorful image processing, which is a new type of ITSs. In the collapse recognition system, image segmentation is a critical and essential component. The roads and slopes are the ROIs in this system.

Roads images segmentation is a process of dividing a natural image including roads into different regions such that each region is, but the union of any two adjacent regions is not,

ISSN: 2005-4254 IJSIP

homogeneous. Various segmentation methods of road images have been proposed [9-11]. Some papers put forward approaches to detect lane and then segment the road based on the lane markings [12-14]. In [15-17] various methods are been proposed to segment the road in the urban environment. However, there are some shortcomings in the methods mentioned in [9-17]: (1) the methods cannot get the roads and slopes at the same time; (2) the algorithms cannot segment the roads or the slopes with collapse exactly; (3) the algorithms always assume that the road is present in the same type, and just suitable for one certain type road; (4) the road images are always taken in a fixed angle, and if the pictures are taken from different angles, the methods will become worse; (5) the algorithms are complex and time-consuming.

Focused on these problems, this paper proposed a novel and effective method to segment the interest regions, *i.e.*, roads and slopes. As we can see in Figure 1 and Figure 2 (positive samples mean roads or slopes with collapse, otherwise the images are negative samples), the images mainly includes buildings, sky, cars, vegetation, which are noise and will be removed. Besides, the road image includes roads and slopes, which are ROIs. The hierarchical approach proposed by this paper does not assume the roads are present in the same type and assume the road images can be captured from arbitrary angles.

This paper is organized as follows. In Section 2, an overview of the proposed segmentation framework is provided. In Section 3, the proposed method is described in details. In Section 4, experimental results and performance of the proposed algorithm are discussed. Section 5 concludes the paper.


**Figure 1. Positive Samples**


**Figure 2. Negative Samples**

 

## 2. Proposed Segmentation Frameworks

Given a road image, the proposed segmentation algorithms work in a hierarchy as presented in Figure 3. Firstly, the vegetation is extracted from the given image. Then we segment the image with K-means clustering based on the feature extracted in L*a*b color space with Gabor filter. After that, the small blobs, such as road signs, cars, buildings are removed based on Max Connected-component Algorithm. This stage includes some post-processing, for example, morphology operation. Lastly, the sky region is separated based on binary image. After the previous processing, the image with roads and slopes can be achieved. We call the proposed framework hierarchical due to its inherent nature, as shown in Figure 3. The detail of the algorithm would be discussed in subsequent sections.

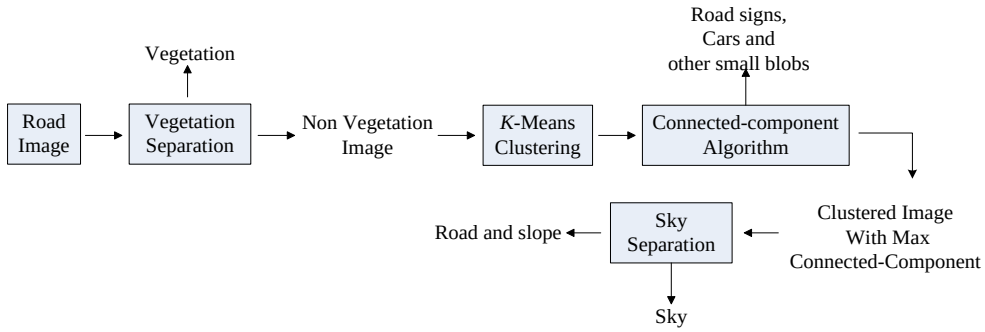


**Figure 3. Proposed Segmentation Framework**

## 3. The Approach of Segmentation

### 3.1. Vegetation Separation

RGB color space is the most commonly used color model. A color image can be decomposed into three components, including Red (R), Green (G), and Blue (B). Generally speaking, for green regions, the value of G is greater than R and B [18]. Therefore, the vegetation can be removed based on the following formula Eq.1:

$$f(i,j) = \begin{cases} 0, & \text{if } G > R \text{ or } G > B \\ 1, & \text{otherwise} \end{cases} \tag{1}$$

Then the images without vegetation can be gotten according to the convolution of $f(i,j)$ and the original image. This paper set the background color of the images to black. The results of this stage are shown in Figure 4 and Figure 5.

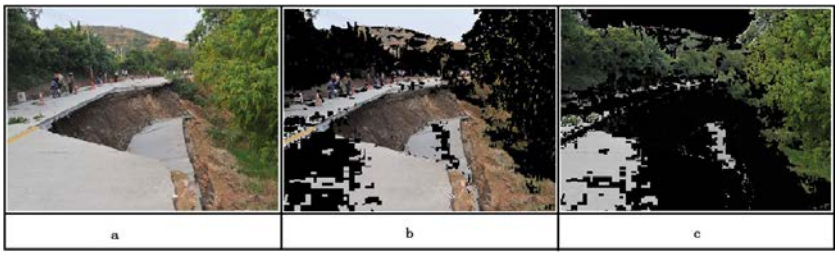


**Figure 4. Vegetation Separation Result of a Positive Sample**
**a: Original Road Image; b: Non Vegetation Image; c: Vegetation Image**

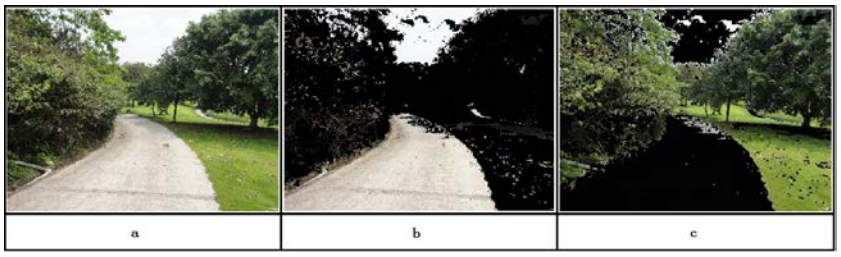


**Figure 5. Vegetation Separation Result of a Negative Sample**
**a: Original Road Image; b: Non vegetation Image; c: Vegetation Image**

As shown in Figure 4, when the vegetation is separated, some parts of the roads have been removed at the same time. In order to solve this problem, we observed the histogram of saturation value in HSI space. Firstly, the image is been transformed to HSI color space based on the following formula (Eq.2, Eq.3, Eq.4).

$$H = \begin{cases} \theta & , \quad B \le G; \\ 360 - \theta, & B > G; \end{cases}$$

$$\text{Where } \theta = \cos^{-1}\left\{\frac{\frac{1}{2}[(R-G)+(R-B)]}{[(R-G)^2+(R-B)(G-B)]^{\frac{1}{2}}}\right\} \tag{2}$$

$$S = 1 - \frac{3}{(R+G+B)}\,[\min(R,G,B)] \tag{3}$$

$$I = \frac{1}{3}(R+G+B) \tag{4}$$

In the HSI color space, the histogram of roads' saturation value can be obtained. By observing the value, the feature of roads is that the saturation value of the road is less than or equal to 0.09, as shown in Figure 6. Based on this feature, we utilize the following formula (Eq.5) to process the images which have been removed the green regions. As it showed in Figure 7.

$$I_R(i,j) = \begin{cases} I_O(i,j), & \text{if } S_{OI}(i,j) \le 0.09 \\ I_G(i,j), & \text{otherwise} \end{cases} \tag{5}$$

Where IO represents the original image, IG stands for the images removed green regions, SOI (i, j) indicates the saturation value of pixel (i, j) in IO, and IR can be obtained by processing the IG using Eq.5.

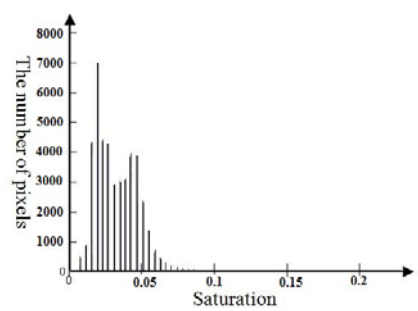


**Figure 6. Histogram of the Road Saturation Value**

 

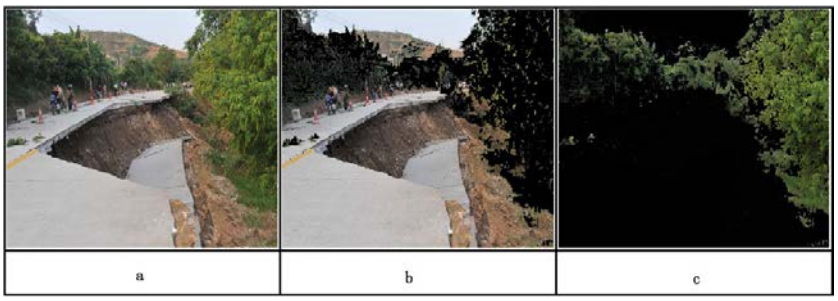


**Figure 7. Post-processed Vegetation Separation Result of a Positive Sample a: Original Image; b: Post-processed Vegetation Image; c: Vegetation Image**

### 3.2. Color Feature Extraction with Gabor Filter

The color feature must be measured before segmentation. To extract features, we compute the response of a Gabor filter oriented at the dominant direction of the neighborhood of a pixel, which is the same as method in[19]. We extract the color feature in the International Commission on Illumination (CIE) L*a*b* space because this color space can independently control color and intensity information. The L*a*b* space consists of a luminosity layer L*, a chromaticity layer a* indicating where color falls along the red–green axis, and a chromaticity layer b* indicating where the color falls along the blue–yellow axis. All of the color information can be extracted in the a* and b* layers without the disturbing of intensity. We consider the local energy content of the a* and b* components as features for image segmentation. Local energy is defined as the method in [20]. The local energy derived for the a* component can be expressed as

$$LE^{a^*}(x,y) = (a^*(x,y) ** G_\theta^o(x,y))^2 + (a^*(x,y) ** G_\theta^e(x,y))^2 \tag{6}$$

Where $G_\theta^o(x,y)$ and $G_\theta^e(x,y)$ are the pair of odd- and even-symmetric filters. The even- and odd-symmetric filters are the real and imaginary parts, respectively, of the complex Gabor filter $G_\theta(x,y)$. Similarly, we can obtain the local energy measurement for the color component b*.

The previous mentioned Gabor filter is employed to extract feature. The filter orients at an angle, which is adaptively chosen for each pixel. The Gabor filter can be defined as follows:

$$G_{f,\theta,\varphi,\sigma}(x,y) = e^{-\frac{x^2+y^2}{2\sigma^2}} e^{j(2\pi f(x\cos\theta + y\sin\theta + \varphi))} \tag{7}$$

Where f is the spatial frequency of the cosine factor, θ is the orientation of the normal to the parallel stripes, φ is the phase offset, and the standard deviation σ of the Gaussian factor determines the (linear) size of the support of the Gabor function. Now, the size of the filter can be related to the standard deviation σ of the Gaussian factor as w =2σ +1. At each pixel, we choose a fixed value of size w, frequency f, and φ phase and a customized value of orientation θ at which the gradients in the local neighborhood possess a dominant direction. There we choose the optimum value of w=7, f=0.1, and φ=0 based on repeated experiments. Then the Gabor filter used in this paper can be expressed with those values as follows:

$$G_\theta(x,y) = e^{-\frac{x^2+y^2}{18}} (\cos\big(0.2\pi(x\cos\theta + y\sin\theta)\big) + j\sin(0.2\pi(x\cos\theta + y\sin\theta))) \tag{8}$$

The orientation of the Gabor filter is determined based on the idea of utilizing the information that is present in the horizontal and vertical gradients, *i.e.*, $\nabla_x$ and $\nabla_y$, respectively. Both gradients are derived by applying the gradient operator on the image. The

orientation angle at pixel (x, y) is determined by following the approach proposed by [21], *i.e.*,

$$\theta_k(x,y) = 90° + \frac{1}{2}\tan^{-1}\left(\frac{2g_{xy}}{g_{xx}-g_{yy}}\right) \tag{9}$$

Where the definitions of $g_{xy}$, $g_{xx}$, and $g_{yy}$ are

$$g_{xy} = \sum_{p=x-(k-1)}^{x+(k-1)} \sum_{q=y-(k-1)}^{y+(k-1)} \nabla_x(p,q)\nabla_y(p,q) \tag{10}$$

$$g_{xx} = \sum_{p=x-(k-1)}^{x+(k-1)} \sum_{q=y-(k-1)}^{y+(k-1)} \nabla_x^2(p,q) \tag{11}$$

$$g_{yy} = \sum_{p=x-(k-1)}^{x+(k-1)} \sum_{q=y-(k-1)}^{y+(k-1)} \nabla_y^2(p,q) \tag{12}$$

### 3.3. K-means Clustering

After the pre-processing to the non vegetation images, we have a set of feature vectors, which extracted by the Gabor filter. To group those pixels, this paper use K-means clustering algorithm. In choosing the number of cluster, the trial-and-error procedure shows that the segmentation result is the best for K=4. For preventing the interference of the background pixels when clustering, a value greater than 255 can be given to the background; this paper set the value as 300. The results displayed in Figure 8 and Figure 9.

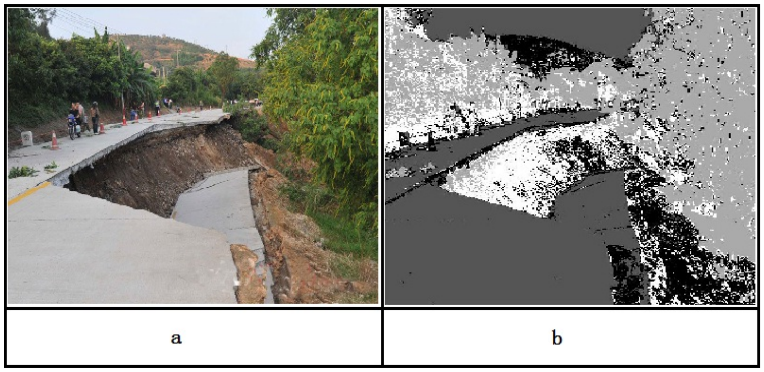


**Figure 8. The Clustered Result of a Positive Sample**
**b is the Clustered Result of Non Vegetation Image based on Image a**

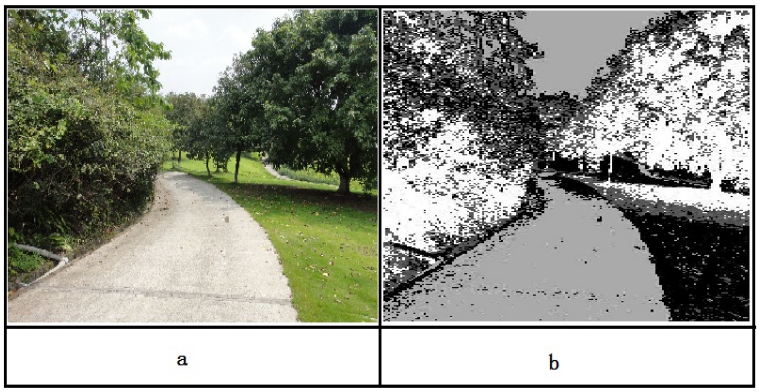


**Figure 9. Clustered Result of a Negative Sample**
**b is the Clustered Result of Non Vegetation Image based on Image a**

 

### 3.4. Road Signs, Cars and Small Blobs Separation

The road images may include some road signs, cars and other small blobs which would be separated based on the size of each part. After clustering, the image is segmented into four categories, including the background. As mentioned above, we set the value of background as 300, so the background can be removed based on the pixel value. Outside the background, three parts has been remained. This paper employed connected-component algorithm to get the max connected-component of each part. The max connected-component is remained for each part. Then we consider the size of each max connected-component. As we all known, the size of road sign and the car is small, and the size of the road and slopes are bigger than them. So some limits are imposed on the size of the max connected-component. The limits for the size criteria are empirically derived by a trial-and-error method based on the experiments on the images. The thresholds for the size criterion are selected at a specific percentage with respect to the size of the images being analyzed. This paper set the threshold as 1/25 of the original image, *i.e.*, the size of road signs, cars and other small blobs is smaller than 1/25 of the original image, roads' and slopes' size are greater than 1/25 of the original image. Based on the threshold, the road signs and small blobs can be separated.

### 3.5. Sky Separation

Once the clustering process and small blobs separation are completed, we obtain several regions including ROIs (roads and slops) and maybe the sky. To get the ROIs, the sky region should be removed. We transform the segmented images to binary images by automatic histogram thresholding segmentation algorithms [22]. The binary images are shown as image b in Figure 11 and Figure 12. We can see that the sky region in the binary images is white, *i.e.*, the value is 1 and it is on the top of the images. In other words, there are adjacent pixels in the first row whose values are all 1. However if the number of the adjacent pixels is small, we will not view it as the sky region. Therefore we set a threshold value for the number of adjacent pixels. We get the threshold value by a trial-and-error method based on the experiments. The limit for the number is chosen as 1/13 of the images' width. According to the features of the sky previously mentioned, the blobs from the clustering stage will be checked. If one of the blobs fit the feature, it is declared as sky. The sky images are shown as image c in the Figure 11and Figure 12. And the process of sky separation is shown in Figure10.

 

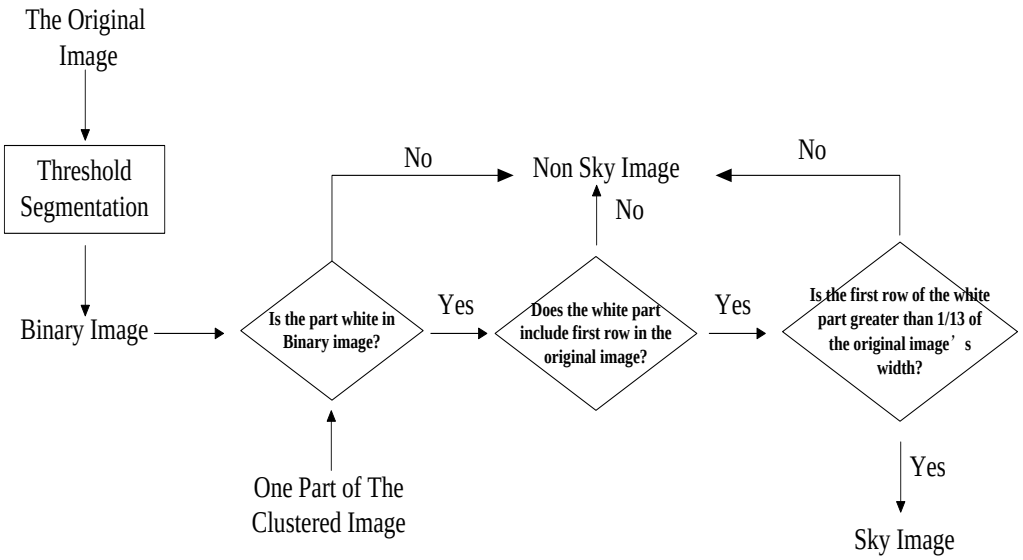


**Figure 10. The Process of Sky Separation**

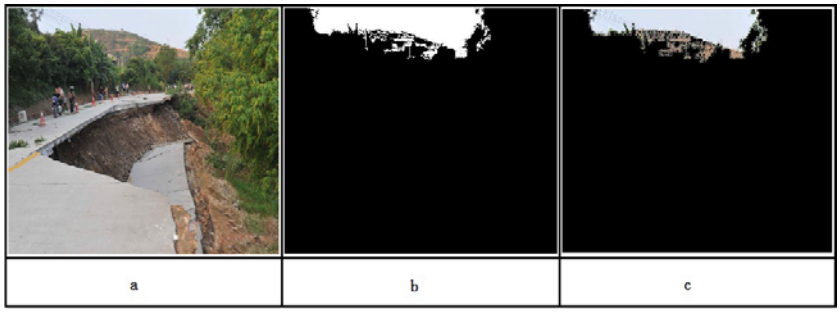


**Figure 11. The Binary Images of Positive Samples**
**a is the Original Image, b is the Binary Image of a, c is Sky Segmented from a**

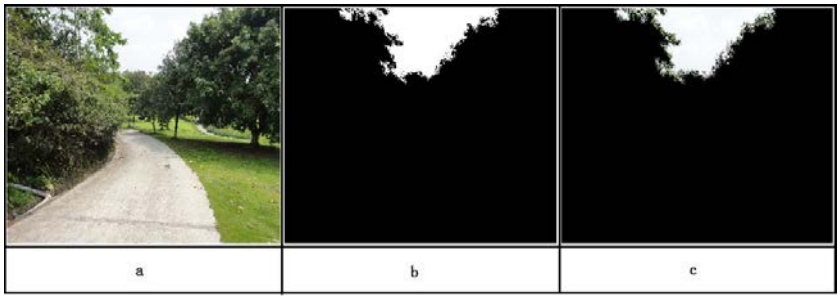


**Figure 12. The Binary Images of Negative Samples**
**a is the Original Image, b is the Binary Image of a, c is Sky Segmented from a**

### 3.6. Road and Slopes

After removing the vegetation, sky, cars, road signs and other small blobs which are noises of the images, the reaming image is declared as road and slope image. We got this conclusion based on the analysis of the road images. To get rid of small scattered colored portions in

 

images, the noise filtering and close operation are applied to the road and slope image which can be seen the results in Figure 13.

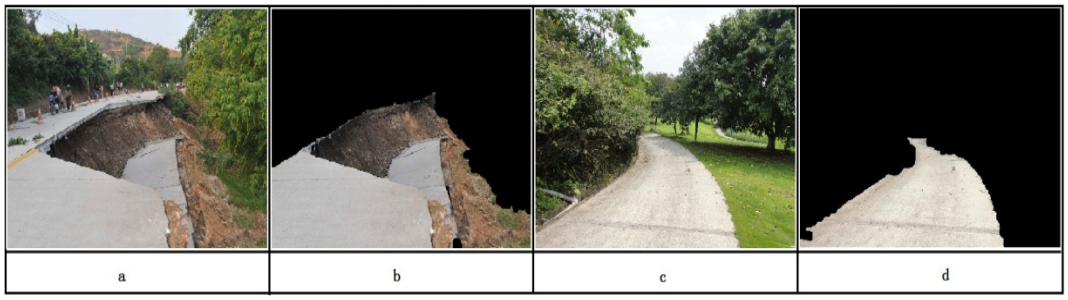


**Figure 13. b is the ROIs Segmented from Image a, d is the ROIs Segmented from Image c**

## 4. Experiment Analyses

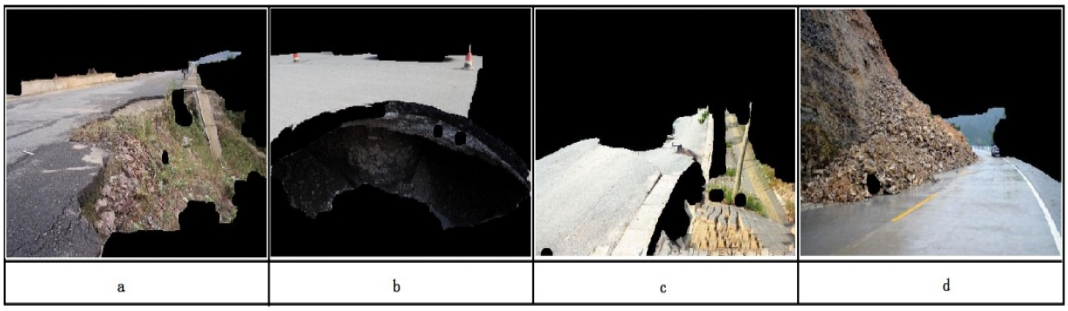


**Figure 14. The Segmentation Results of Representative Positive Road Images**

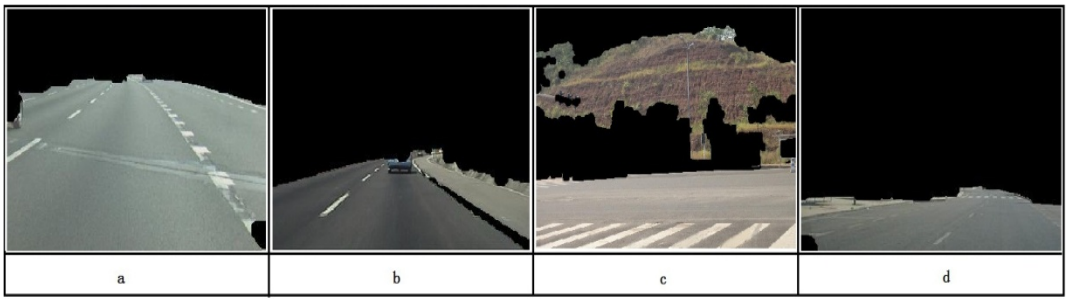


**Figure 15. The Segmentation Results of Representative Negative Road Images**

To evaluate the proposed approach, we have performed experiments on a large collection of images, where some test images are obtained from LabelMe database and Google Image, the other images provided by the project team, and the rest are captured by us. Because the segmentation method would be applied in recognition of roads and slopes collapse system, so the experiment must be done on various images containing roads and slopes that with and without collapse. Figure 14 and Figure 15 showed the results of representative positive and negative samples. These figures show that our method can achieve very good result. In Figure 14, the images are roads and slopes with collapse, and the road images are complex. The roads are unstructured, which are more complex than the structured roads. The segmented results show our approach is suitable for both unstructured and structured road images. In

 

Figure 15 we can see samples without collapse, and those photos were taken from different angles, such as b is different from others; and (a) and (d) are with a bad quality because of the light. However most of the results are satisfied and can get the ROIs accurately. All in all, the approach is suitable for the segmentation of various roads and slopes, and the results are excellent. It is worth noting that the proposed approach is efficient, which runs once for 2.08 seconds on the image that is 320k bits.

All in all, the hierarchical approach proposed by this paper is efficient and can segment the roads and slopes in the same time. Besides, it is suitable for various road images, no matter the roads are structured or unstructured, the roads and slopes are with or without collapse, the images are with good quality or not, and the images are taken from which angle. Most importantly, the method can get a satisfied result.

Above all, some criterions are introduced to compare the segment results. 1270 images selected from LableMe database [23], Google images and from other sources.

(1) Correctly segment the ROI (CSR): a segmented region that contains ROIs and little background.

(2) Falsely segmented the ROI (FSR): a segmented region that does not contain ROIs or complete ROIs, or the background holds a large proportion in the segmented region.

(3) Precision rate (PR): PR= CDR/ (CDR+FDR).

The results are showed in Table 1.The precision rate proved that the method proposed in this paper can get a satisfied result. And the results show that the algorithm is more suitable for suburbs roads detection without buildings.

**Table 1. Results of the Method in this Paper**

| | Total number of road images | CSR | FSR | PR |
|---|---|---|---|---|
| The Hierarchical Segmentation Approach | 1270 | 1135 | 135 | 89.37% |

## 5. Conclusions

This paper has presented a new way to segmentation roads and slopes, which is the first and key step for the recognition of collapse. Different from previous approaches, our method is suitable for the segmentation of various roads and slopes images and can get a satisfied result. Besides, it is efficient so that it can be used in the real-time system. The application of our methods is novel which is a new type of ITS. Experimental results show a superior ability of our method to improve the segmentation quality with a low computational cost. In future research on this topic, we will consider the following issues. First, we will incorporate more image attributes as features. Second, more post-processing algorithms will be used to improve the quality of the segmented image.

## Acknowledgements

We are very thanks to the anonymous reviewers for their useful comments. The works is supported by the project of Science and Technology Project of Ministry of Transport under Grant No. 2011318740240, and the Chongqing key scientific and technological project under the No. CSTC 2010AB2001.

 

## References

[1] F. Oniga, R. Danescu and S. Nedevschi, "Mixed road surface model for driving assistance systems", IEEE International Conference on Intelligent Computer Communication and Processing, Cluj-Napoca, Romania, **(2010)** August 26-28..

[2] F. Oniga, S. Nedevschi, M. M. Meinecke and T. B. To, "Road Surface and Obstacle Detection Based on Elevation Maps from Dense Stereo", IEEE conference on Intelligent Transportation Systems, Proceeding, Seattle, US, **(2007)** September 30-October 3.

[3] A. Seki and M. Okutomi, "Robust Obstacle Detection in General Road Environment Based on Road Extraction and Pose Estimation", Electron Commun Jpn Part II Electron, vol. 12, no. 90, **(2007)**.

[4] J. Pangyu and S. Nedevschi, "Obstacle detection based on the hybrid road plane under the weak calibration conditions", IEEE Intelligent Vehicles Symposium, Eindhoven, Netherlands, **(2008)** June 4-6.

[5] A. Tsukada, M. Ogawa and F. Galpin, "Road structure based scene understanding for intelligent vehicle systems", International Conference on Intelligent Robots and Systems, Taipei, Taiwan, **(2010)** October 18-22.

[6] J. Zavadil, J. Tuma and V. M. F. Santos, "Traffic signs detection using blob analysis and pattern recognition", 13th International Carpathian Control Conference, High Tatras, Slovakia, **(2012)** May 28-31.

[7] H. Oliveira and P. L. Correia, "Automatic Road Crack Detection and Characterization", IEEE Transactions on Intelligent Transportation Systems, vol. 99, **(2012)**.

[8] W. Wei, L. Boying and B. Peng, "Automatic Road Crack Image Preprocessing for Detection and Identification", Second International Conference on Intelligent Networks and Intelligent Systems, Tianjin, China, **(2009)** November 1-3.

[9] K. Hui, J. Y. Audibert and J. Ponce, "General Road Detection From a Single Image", IEEE Transactions on Image Processing, vol. 19, no. 8, **(2010)**.

[10] M. Mazaheri and S. Mozaffari, "Real time adaptive background estimation and road segmentation for vehicle classification", 19th Iranian Conference on Electrical Engineering, Tehran, Iran, **(2011)** May 17-19.

[11] D. B. Lewis, J. M. Keller, M. Popescu and K. Stone, "Dirt road segmentation using color and texture features in color imagery", IEEE Symposium on Computational Intelligence for Security and Defence Applications, Ottawa, Canada, **(2012)** July 11-13.

[12] Y. Sebsadji, J. P. Tarel, P. Foucher and P. Charbonnier, "Robust road marking extraction in urban environments using stereo images", IEEE Intelligent Vehicles Symposium, La Jolla, US, **(2010)** June 21-24.

[13] F. M. Sebdani and H. Pourghassem, "A robust and real-time road line extraction algorithm using hough transform in intelligent transportation system application", IEEE International Conference on Computer Science and Automation Engineering, Zhangjiajie, China, **(2012)** May 25-27.

[14] L. Zhao, C. Zixing, X. Jin and R. Xiaoping, "Road markings extraction based on threshold segmentation", 9th International Conference on Fuzzy Systems and Knowledge Discovery, Chongqing, China, **(2012)** May 29-31.

[15] Z. Geng, Z. Nanning, C. Chao, Y. Yuzhen and Y. Zejian, "An efficient road detection method in noisy urban environment", IEEE Intelligent Vehicles Symposium, Xi'an, China, **(2009)** June 3-5.

[16] M. Suzuki, T. Saitoh, E. Terada and Y. Kuroda, "Online road segmentation for urban complex environments", International Symposium on Communications and Information Technologies, Tokyo, Japan, **(2010)** October 26-29.

[17] Z. Wang and B.G. Cai, "A ROI setting method for vehicle detection in urban environment", IEEE-APS Topical Conference on Antennas and Propagation in Wireless Communications, Cape Town, South Africa, **(2012)** September 2-7.

[18] J. Guo-Quan, Z. Cui-Jun and Q. Jun-Yan, "The research of image segmentation based on color characteristic", International Conference on Machine Learning and Cybernetics, Guilin, China, **(2011)** July 10-13.

[19] Y. Kang, K. Yamaguchi, T. Naito and Y. Ninomiya, "Multiband Image Segmentation and Object Recognition for Understanding Road Scenes", IEEE Transactions on Intelligent Transportation Systems, vol. 12, no. 4 **(2011)**.

[20] M. C. Morrone and D. C. Burr, "Feature detection in human vision: A phase-dependent energy model", Proceedings of the Royal Society B-Biological Sciences, vol. 235, no. 1280, **(1988)**.

 

## Authors

**Yuanyuan Jia**, she is currently a PhD student in College of Computer Science in Chongqing University, China. She received his B.S. degree in Computer Science and Technology, Hebei Normal University, 2010. She is doing a combined Master-PhD program since 2010.Her major interests are in the field of image processing.

**Zhongshi He**, he is a professor in College of Computer Science of Chongqing University. He is the vice-president of College of Computer Science. His research interests are machine learning, pattern recognition, image processing and natural language processing.

**Huazheng Zhu**, he received the B.Sc. degree in mathematical and computer science from Gannan Normal University, Ganzhou, China, in 2008, and then M.Sc. degree in mathematical and computer science from Guangxi University for Nationalities, Nanning, China, in 2011. He is currently pursuing the PH.D. degree in computer science, Chongqing University, Chongqing, China. His main research interests include evolutionary optimization in bioinformatics.

 